Undamped Modal Analysis: From Theory to Finite Element Practice

Dr. Iman Salehinia
Associate Professor of Mechanical Engineering
Northern Illinois University, DeKalb, USA

May 16, 2025

Watch MechCADemy Video: Theory of FEA

Your support matters! Please **Subscribe** to MechCADemy YouTube channel, share the videos with others, and let me know your comments and suggestions to help improve future content.

Contents

1 Introduction; General Equation of Motion

Modal analysis is one of the most fundamental dynamic analyses in mechanical and structural engineering. It is used to determine the vibration characteristics of linear elastic structures, specifically their natural frequencies and corresponding mode shapes. These results form the foundation for many other dynamic simulations.

In the world of engineering design and analysis, understanding how structures respond to dynamic forces is just as critical as analyzing their behavior under static loads. Modal analysis provides a powerful means of gaining this dynamic insight. Every physical structure—from a tiny microchip to a towering skyscraper—has certain natural frequencies at which it tends to vibrate. When these natural frequencies are excited—by wind, machinery, traffic, or seismic activity—the resulting amplified vibrations can lead to fatigue, performance degradation, or even catastrophic failure.

Through modal analysis, engineers can:

- Identify critical frequencies that must be avoided during operation.
- Guide design modifications to shift natural frequencies away from external excitations.
- Optimize mass and stiffness distribution for improved dynamic performance.
- Develop more accurate dynamic models for use in further analyses such as transient dynamics or harmonic response studies.

Even if a structure is not expected to experience significant dynamic loads during its operational lifetime, **modal analysis remains essential**. Across industries such as aerospace, automotive, civil, energy, electronics, and manufacturing, regulatory standards often mandate modal testing or simulation to ensure that designs are safe against vibration-induced failures.

For instance, the **MIL-STD-810H** standard, widely used in the defense sector, outlines procedures for environmental engineering considerations and laboratory testing. Specifically, **Method 514.8** addresses vibration testing to evaluate the performance, structural integrity, and durability of equipment when subjected to vibration during transport, handling, and operational conditions [1].

Similarly, the **IEC 60068-2-6** standard specifies procedures for sinusoidal vibration testing. It defines a method for subjecting specimens to sinusoidal vibrations over a specified frequency range to identify mechanical weaknesses or performance degradation [2].

Moreover, even if devices or structures are not subjected to dynamic loading during their operation, they often need to be transported from the assembly site to the field. Transportation can introduce a range of vibrational forces that may coincide with the natural frequencies of the structure, leading to resonance and potential damage. Modal analysis is crucial in these scenarios to ensure that the design can withstand such conditions.

For example, during the transportation of sensitive equipment, understanding the modal characteristics allows engineers to design appropriate packaging and support structures that mitigate the risk of resonance-induced failures. This proactive approach is vital to maintain the integrity and functionality of the equipment upon arrival at its destination.

The reader is also encouraged to consult the *"PIP-II HB650 Cryomodule Transportation Design Report"*, prepared by Fermi National Accelerator Laboratory. This document discusses practical design considerations for transporting highly sensitive accelerator components and highlights how modal analysis plays a critical role in ensuring safe delivery. One of the report's authors is my former graduate student, Mr. Josh Helsper. The report can be accessed at:

https://indico.fnal.gov/event/55397/contributions/246409/attachments/157651/206360/2020_10_26_HB650_Transportation_Design_Report_JFH_.pdf

Moreover, modal analysis helps engineers develop a deeper, dynamic understanding of their designs. It reveals how shape, material properties, and boundary conditions influence a system's vibrational behavior. These insights contribute to designs that are not only strong but also robust, efficient, and long-lasting.

Other types of dynamic analyses—such as harmonic analysis, transient dynamic analysis, random vibration analysis, and response spectrum analysis—often rely on the results of modal analysis as critical input. By using the natural frequencies and mode shapes computed from modal analysis, these simulations can be significantly simplified and accelerated.

In the context of Finite Element Analysis (FEA), modal analysis allows engineers to predict the dynamic behavior of structures virtually, early in the design phase. This reduces the need for costly prototypes and extensive physical testing. By integrating FEA with modal analysis, engineers can explore multiple design iterations quickly, optimize performance, and ensure reliability before a product reaches production.

We begin with the general equation of motion and its reduction to the undamped eigenvalue form, then ground the theory with hand-worked spring–mass examples that show every algebraic step. Next, the notes introduce pre-stress effects and geometric stiffness, explaining how initial loads shift natural frequencies. The discussion then transitions to finite-element practice: how mass matrices are assembled, why consistent versus lumped forms matter, and which numerical solvers (Lanczos, sub-space iteration) are favoured for large, sparse models.

The closing pages gather key take-aways and supply worked finite-element benchmarks so readers can test the workflows on their own.

Modal analysis is a linear dynamic analysis, based on solving the general equation of motion, where the unknowns are the acceleration, velocity, and displacement at all points over the structure. The general equation of motion for a dynamic system is

$$\mathbf{M}\,\ddot{\mathbf{u}}(t) + \mathbf{C}\,\dot{\mathbf{u}}(t) + \mathbf{K}\,\mathbf{u}(t) = \mathbf{f}(t), \tag{1.1}$$

where $\mathbf{M}$ is the mass matrix, $\mathbf{C}$ the damping matrix, $\mathbf{K}$ the stiffness matrix, $\mathbf{u}$ the displacement vector, and $\mathbf{f}(t)$ the external load vector [3, 4, 5, 6, 10].

For modal analysis we impose two simplifications:

1. The external dynamic load $\mathbf{f}(t)$ is set to zero because natural frequencies and mode shapes are intrinsic properties of the structure and are independent of external excitation.

   In classical (no-preload) modal analysis, the structure is assumed to be free from external static or dynamic loading during the extraction of modes.

In pre-stressed modal analysis, while $\mathbf{f}(t)$ is still set to zero for modal extraction, the presence of initial static stresses modifies the effective stiffness through a geometric stiffness matrix, influencing the computed natural frequencies and mode shapes.

2. Damping is neglected because including it introduces complex numbers and complicates the analysis. At this stage, we are interested in the undamped natural frequencies and mode shapes, which provide the fundamental dynamic characteristics of the structure.

With these assumptions the equation reduces to

$$\mathbf{M}\,\ddot{\mathbf{u}}(t) + \mathbf{K}\,\mathbf{u}(t) = \mathbf{0}. \tag{1.2}$$

2 Derivation of the Eigen-Value Problem

In this section, we present the derivation of the eigen-value problem for both single degree of freedom (SDOF) and multiple degrees of freedom (MDOF) systems. We begin by formulating the governing differential equation for an SDOF system, then generalize the concept to MDOF systems. Finally, we explain the rationale behind assuming a harmonic form of the solution, which simplifies the problem and leads to a well-defined mathematical structure for extracting natural frequencies and mode shapes.

2.1 Single Degree of Freedom (SDOF) System

For a spring-mass system with mass m and stiffness k, the equation of motion is:

$$m\ddot{u}(t) + ku(t) = 0.$$

Assume a harmonic solution:

$$u(t) = A\sin(\omega t + \theta).$$

Substituting into the equation of motion:

$$-m\omega^2 A\sin(\omega t + \theta) + kA\sin(\omega t + \theta) = 0,$$

which simplifies to:

$$(k - m\omega^2)A = 0.$$

For a non-trivial solution ($A \neq 0$), the term in parentheses must vanish:

$$\boxed{k - m\omega^2 = 0} \quad \Rightarrow \quad \boxed{\omega = \sqrt{\frac{k}{m}}}. \tag{2.1}$$

Thus, for a SDOF system, the eigenvalue problem simply reduces to finding the natural frequency ω. This is a very important and powerful formula! It provides valuable insight into how geometry and mass affect natural frequency. For example, a very tall skyscraper has a large mass, which can lead to low natural frequencies. Similarly, between two beams with the same cross-section and material density, the longer beam will have lower natural frequencies because it has a smaller stiffness (due to increased flexibility) and greater mass.

$$\boxed{\text{The unit of } \omega \text{ is s}^{-1} \text{ (radians per second)}}$$

Note that this is the angular (circular) frequency. The corresponding frequency in hertz (cycles per second) is given by:

$$\boxed{f = \frac{\omega}{2\pi} \quad \text{with units of Hz (cycles per second)}}$$

2.2 Multiple Degrees of Freedom (MDOF) System

For an n-DOF system, the equations of motion are written in matrix form:

$$M\ddot{\boldsymbol{u}}(t) + K\boldsymbol{u}(t) = 0,$$

where:

- M is the mass matrix,
- K is the stiffness matrix,
- $\boldsymbol{u}(t)$ is the displacement vector.

Assume a modal expansion for the displacement:

$$\boldsymbol{u}(t) = \sum_{i=1}^{n} \boldsymbol{\Phi}_i \, q_i(t),$$

where each modal coordinate $q_i(t)$ is given by:

$$q_i(t) = A_i \sin(\omega_i t + \theta_i).$$

Substituting into the equation of motion:

$$M \sum_{i=1}^{n} \boldsymbol{\Phi}_i \, \ddot{q}_i(t) + K \sum_{i=1}^{n} \boldsymbol{\Phi}_i \, q_i(t) = 0.$$

Since $\boldsymbol{\Phi}_i$ are time-independent, and differentiating $q_i(t)$ twice gives:

$$\ddot{q}_i(t) = -\omega_i^2 A_i \sin(\omega_i t + \theta_i) = -\omega_i^2 q_i(t),$$

we substitute:

$$M \sum_{i=1}^{n} \boldsymbol{\Phi}_i(-\omega_i^2 q_i(t)) + K \sum_{i=1}^{n} \boldsymbol{\Phi}_i q_i(t) = 0.$$

Grouping terms:

$$\sum_{i=1}^{n} (K - \omega_i^2 M)\boldsymbol{\Phi}_i q_i(t) = 0.$$

For nontrivial $q_i(t)$, each term must individually satisfy:

$$\boxed{(K - \omega_i^2 M)\mathbf{\Phi}_i = 0}. \tag{2.2}$$

This is the generalized eigenvalue problem for each mode.
To find nontrivial solutions, we require:

$$\boxed{\det(K - \omega_i^2 M) = 0}.$$

Solving this equation provides:

- Eigenvalues ω_i^2 (squared natural frequencies),
- Eigenvectors $\mathbf{\Phi}_i$ (mode shapes).

2.3 Why Assume a Harmonic Solution?

For undamped free vibration, the system is governed by linear, second-order differential equations with constant coefficients:

$$M\ddot{\mathbf{u}}(t) + K\boldsymbol{u}(t) = 0.$$

The general solution to such equations involves exponential functions [4, 5, 6]:

$$\boldsymbol{u}(t) = C_1 e^{\lambda_1 t} + C_2 e^{\lambda_2 t},$$

where λ_1 and λ_2 are roots of the characteristic equation.
For undamped systems, $\lambda_{1,2} = \pm i\omega$, leading to purely imaginary roots. Thus,

$$e^{i\omega t} = \cos(\omega t) + i\sin(\omega t),$$

and the real part represents harmonic motion.
Hence, the natural form of the solution is harmonic:

$$\boldsymbol{u}(t) = A\sin(\omega t + \theta). \tag{2.3}$$

2.4 Alternative Assumptions

Assumed Solution	**Physical Meaning**	**Correct for Undamped Vibration?**
$A\sin(\omega t + \theta)$	Harmonic oscillation	Yes
$e^{i\omega t}$	Complex form of oscillation	Yes
$e^{\lambda t}$ (real λ)	Exponential growth/decay	No
Polynomial $(a + bt + ct^2)$	Non-oscillatory	No

Thus, assuming non-harmonic solutions (e.g., polynomials) leads to either trivial or physically incorrect results.

2.5 Spatial vs. Temporal Phase: Mode Shape and Phase Angle

In practice, it is easy to blur the distinction between a *mode shape*—which governs the *spatial* pattern of vibration—and the *phase angle* that shifts that pattern in *time*. Some references even seem to treat the two notions interchangeably, which can cloud a clear physical interpretation of modal results.

Because this mix-up can hinder a correct physical interpretation of modal results, the next subsection disentangles these two notions and illustrates the difference with concrete cantilever-beam examples.

The complete displacement field of a single real (undamped) mode is

$$u(x,t) = A\,\phi(x)\,\sin\bigl(\omega t + \theta\bigr), \tag{2.4}$$

where

- $\phi(x)$ is the *mode shape*—a purely **spatial** function fixed by the eigen-value problem $(K - \omega^2 M)\phi = 0$;
- θ is one global *phase angle* that shifts the motion **in time** and is determined only by initial conditions;
- A sets the overall amplitude.

In-phase and out-of-phase motion inside one real mode. For any two degrees of freedom j and k

$$\frac{u_j(t)}{u_k(t)} = \frac{\phi_j}{\phi_k}\,. \tag{2.5}$$

Hence

- If ϕ_j and ϕ_k have the *same sign*, their time histories are identical up to a scale factor $\Rightarrow 0°$ phase difference (*in-phase*).
- If the signs are *opposite*, one trace is $-\sin(\ldots) = \sin(\ldots + \pi) \Rightarrow 180°$ phase difference (*out-of-phase*).

The decision is encoded entirely in the *sign pattern of the mode shape*; the global θ never alters these internal relations.

Examples—cantilever beam.

1. **First bending mode.** $\phi_1(x) > 0$ along the span; every point reaches peaks and zero-crossings simultaneously. The whole beam vibrates in-phase, regardless of the chosen θ.
2. **Second bending mode.** $\phi_2(x)$ changes sign at one interior node. Points on the root–node side ($\phi_2 > 0$) are 180° out-of-phase with points on the node–tip side ($\phi_2 < 0$). The node itself ($\phi_2 = 0$) remains stationary. Again, θ only slides the entire movie left or right in time.

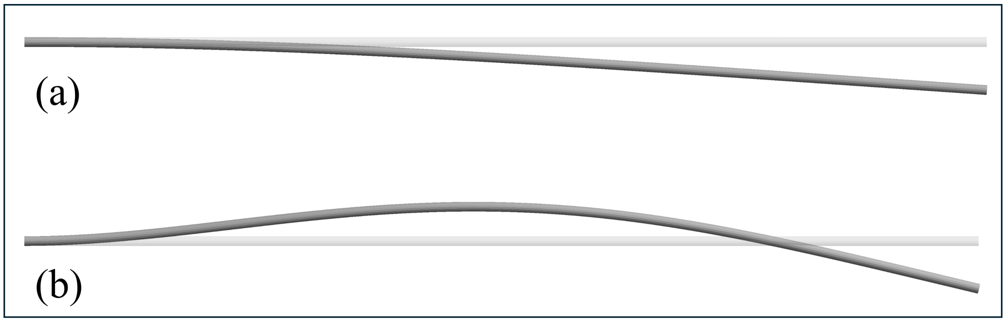

Figure 1: (a) 1st and (b) 2nd bending modes for a cantilevered beam

What the phase angle θ can and cannot do.

- *Can:* act as a common clock offset $t_0 = \theta/\omega$ for the *entire* mode; it is fixed by the initial displacement/velocity projections onto that mode.
- *Cannot:* create additional point-to-point phase lags inside the same real mode.

Take-away: **Mode shape chooses the choreography (who moves with whom and who opposes whom); the global phase angle chooses the curtain-up time.**

3 Worked Lumped-Mass Examples-FEA Approach

To bridge the gap between theory and practical application, this section presents worked examples using a lumped-parameter modeling approach within the finite element analysis (FEA) framework. These examples demonstrate how mass and stiffness matrices can be constructed manually for discrete mechanical systems and how the resulting eigen-value problem can be solved to determine natural frequencies and mode shapes. By working through these examples step-by-step, students can gain a deeper understanding of how FEA concepts apply to real-world dynamic systems, especially when dealing with simplified models where the structure is represented by discrete masses and springs.

3.1 Example 1: Single-Mass (2 DOFs)

Physical Model:

A single spring and mass system:

- Node 0: Fixed (Ground)
- Node 1: Mass $m = 2\,\mathrm{kg}$
- Spring $k = 18\,\mathrm{N/m}$ between Node 0 and Node 1

Element Stiffness Matrix:

$$K_e = k \begin{bmatrix} 1 & -1 \\ -1 & 1 \end{bmatrix}$$

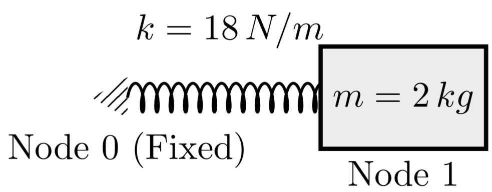

Figure 2: one-mass system

Global Stiffness Matrix (before BCs):

$$K = \begin{bmatrix} 18 & -18 \\ -18 & 18 \end{bmatrix}$$

Global Mass Matrix:

$$M = \begin{bmatrix} 0 & 0 \\ 0 & 2 \end{bmatrix}$$

(Only Node 1 has mass; Node 0 is fixed.)

Boundary Conditions:

- Node 0 fixed → eliminate first row and column.

Reduced Matrices:

$$K_{\text{red}} = [18], \quad M_{\text{red}} = [2]$$

Eigenvalue Problem:

$$(K_{\text{red}} - \omega^2 M_{\text{red}})\Phi = 0$$

$$18 - 2\omega^2 = 0 \quad \Rightarrow \quad \omega^2 = 9 \quad \Rightarrow \quad \omega = 3\,\text{rad/s}$$

Mode Shape:

$$\Phi = [1]$$

3.2 Example 2: Two-Mass (4 DOFs)

Physical Model:

Two masses connected by springs:

- Node 0: Fixed (Ground)
- Node 1: Mass $m_1 = 2\,\text{kg}$
- Node 2: Mass $m_2 = 1\,\text{kg}$
- Node 3: Fixed (Ground)
- Springs:
  - $k_1 = 30\,\text{N/m}$ between Node 0 and Node 1
  - $k_2 = 20\,\text{N/m}$ between Node 1 and Node 2

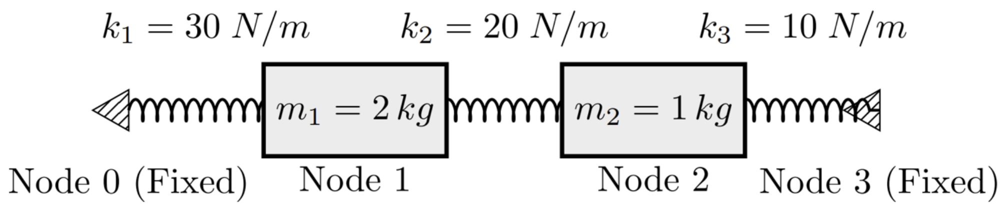

Figure 3: Two-mass system

– $k_3 = 10\,\text{N/m}$ between Node 2 and Node 3

Element Stiffness Matrix for each spring:

$$K_e = k_e \begin{bmatrix} 1 & -1 \\ -1 & 1 \end{bmatrix}$$

Global Stiffness Matrix (before BCs):

$$K = \begin{bmatrix} 30 & -30 & 0 & 0 \\ -30 & 50 & -20 & 0 \\ 0 & -20 & 30 & -10 \\ 0 & 0 & -10 & 10 \end{bmatrix}$$

Global Mass Matrix:

$$M = \begin{bmatrix} 0 & 0 & 0 & 0 \\ 0 & 2 & 0 & 0 \\ 0 & 0 & 1 & 0 \\ 0 & 0 & 0 & 0 \end{bmatrix}$$

Boundary Conditions:

- Nodes 0 and 3 are fixed $\rightarrow$ eliminate rows and columns 0 and 3.

Reduced Matrices:

$$K_{\text{red}} = \begin{bmatrix} 50 & -20 \\ -20 & 30 \end{bmatrix}, \quad M_{\text{red}} = \begin{bmatrix} 2 & 0 \\ 0 & 1 \end{bmatrix}$$

Eigenvalue Problem:

$$(K_{\text{red}} - \omega^2 M_{\text{red}})\Phi = 0$$

Expanding:

$$\det \begin{bmatrix} 50 - 2\omega^2 & -20 \\ -20 & 30 - \omega^2 \end{bmatrix} = 0$$

Solving:

$$2\omega^4 - 110\omega^2 + 1100 = 0$$

note that this is called the "characteristic equation" for the system.

$$\omega_1 = 3.626\,\text{rad/s}, \quad \omega_2 = 6.472\,\text{rad/s}$$

Mode Shapes (relative):

$$\Phi^{(1)} \approx \begin{bmatrix} 0.843 \\ 1 \end{bmatrix}, \quad \Phi^{(2)} \approx \begin{bmatrix} -0.593 \\ 1 \end{bmatrix}$$

To make sure, you understand how mode shapes are calculated, please see below the detailed calculation of the 2nd mode shape.

To compute the second mode shape, we solve the eigenvalue problem:

$$(\mathbf{K} - \omega^2 \mathbf{M})\boldsymbol{\phi} = \mathbf{0}$$

Using the previously computed second eigenvalue $\omega_2^2 \approx 41.86$, we construct the matrix:

$$\mathbf{K} - \omega_2^2 \mathbf{M} = \begin{bmatrix} 50 & -20 \\ -20 & 30 \end{bmatrix} - \begin{bmatrix} 2 & 0 \\ 0 & 1 \end{bmatrix} (41.86) = \begin{bmatrix} 50 - 2(41.86) & -20 \\ -20 & 30 - 41.86 \end{bmatrix} = \begin{bmatrix} -33.72 & -20 \\ -20 & -11.86 \end{bmatrix}$$

We now solve:

$$\begin{bmatrix} -33.72 & -20 \\ -20 & -11.86 \end{bmatrix} \begin{bmatrix} \phi_1 \\ \phi_2 \end{bmatrix} = \begin{bmatrix} 0 \\ 0 \end{bmatrix}$$

From the first row:

$$-33.72\phi_1 - 20\phi_2 = 0 \quad \Rightarrow \quad \frac{\phi_1}{\phi_2} = -\frac{20}{33.72} \approx -0.593$$

Thus, a valid (unnormalized) mode shape for the second mode is:

$$\boxed{\boldsymbol{\phi}_2 = \begin{bmatrix} -0.593 \\ 1 \end{bmatrix}}$$

This indicates that the two masses move in opposite directions (out of phase), with mass 1 moving at a smaller amplitude than mass 2.

Note that mode shapes show the relative deformation (configuration) of a structure at the associated natural frequency, not the absolute values of the deformation.

Furthermore, the total number of mode shapes in a system equals the number of free (unconstrained) degrees of freedom (DOFs). For instance, if a discretized model of a flying drone has one million unconstrained DOFs (also called free-free), there will be one million corresponding mode shapes. The first six modes will have natural frequencies equal to zero, representing the entire system's rigid body motions: three translations and three rotations.

In general, for every free or disconnected component in a finite element (FE) model that is not constrained or properly connected to the rest of the structure, there will be zero (or near-zero) natural frequencies. These zero-frequency modes serve as a useful diagnostic tool: if the number of rigid body modes is greater than expected, it may indicate that parts of the model are unintentionally floating or disconnected. Thus, checking for zero-frequency modes can help verify whether the FE model has been correctly defined and assembled.

3.3 How is u(t) calculated at any time?

A good question that might be in your mind is that, knowing natural frequencies and mode shapes, how do we find the positions/displacements at any time?

Assumed modal coordinates

$$q_1(t) = 2\sin(3.626\,t), \qquad q_2(t) = 0.5\sin(6.472\,t)$$

Mode-shape matrix

$$\mathbf{\Phi} = \begin{bmatrix} 0.843 & -0.593 \\ 1 & 1 \end{bmatrix} = \begin{bmatrix} \boldsymbol{\phi}^{(1)} & \boldsymbol{\phi}^{(2)} \end{bmatrix}$$

Total displacement vector

$$\mathbf{u}(t) = \mathbf{\Phi} \begin{bmatrix} q_1(t) \\ q_2(t) \end{bmatrix} \quad \Longrightarrow \quad \begin{cases} u_1(t) = 0.843\,q_1(t) - 0.593\,q_2(t) \\ u_2(t) = q_1(t) + q_2(t) \end{cases}$$

Evaluation at $t = 1$ s

$$\begin{aligned} q_1(1) &= 2\sin(3.626) = 2(-0.465) \approx -0.931, \\ q_2(1) &= 0.5\sin(6.472) = 0.5(0.188) \approx 0.0938. \end{aligned}$$

$$\begin{aligned} u_1(1) &= 0.843(-0.931) - 0.593(0.0938) = -0.785 - 0.0554 \approx \boxed{-0.841\text{ m}}, \\ u_2(1) &= -0.931 + 0.0938 \approx \boxed{-0.838\text{ m}}. \end{aligned}$$

Final displacements at $t = 1$ s

$$u_1(1) = -0.841\text{ m}, \qquad u_2(1) = -0.838\text{ m}.$$

4 Pre-Stress Modal Analysis

In many practical applications, structures operate under significant static loads before experiencing dynamic excitations. Examples include bridges under dead weight, aircraft wings under aerodynamic lift, and rotating components under centrifugal forces. These initial static loads introduce stress distributions throughout the structure, which in turn alter its dynamic behavior.

When a structure carries an initial (pre-)stress, the usual linear vibration problem is modified by an extra stiffness term. This *geometric stiffness* (also called initial-stress or stress-stiffening matrix, K_g) arises from linearizing the equilibrium about a pre-stressed state. In finite-element form, one finds the total linearized stiffness as the sum of the material (elastic) stiffness K_e and the geometric stiffness K_g [7, 8, 9].

For a general continuum element, K_e and K_g can be written as energy integrals:

$$K_e = \int_\Omega B^T D B \, d\Omega, \quad K_g = \int_\Omega B_\sigma^T \, \sigma^0 \, B_\sigma \, d\Omega, \tag{4.1}$$

where B is the strain-displacement matrix (relating nodal displacements to strains) and B_σ arises from derivatives of the shape functions in the current configuration. Here σ^0 is the initial (Cauchy) stress tensor in the element from the pre-loading.

The geometric stiffness depends on the initial stress distribution but not on the elastic modulus (except through the stress). It can stiffen or soften the structure.

4.1 Physical Interpretation and Impact on Modes

Physically, geometric stiffness reflects how an initial tension or compression affects small vibrations. A common analogy is a taut string or beam: tension makes it stiffer to transverse deflection, while compression makes it more flexible (tending toward buckling). In modal terms:

- **Tensile pre-stress** ($\sigma^0 > 0$) *increases* the natural frequencies.
- **Compressive pre-stress** ($\sigma^0 < 0$) *decreases* the natural frequencies.

These effects enter the eigenproblem through K_g. The total stiffness matrix becomes $K_e + K_g$. If K_g has negative contributions (as with compression), it can reduce the positive-definiteness of K_e. As compressive loading approaches the buckling limit, some eigenvalues ω^2 approach zero.

Thus, pre-stressed structures satisfy:

$$(K_e + K_g)\, \phi = \omega^2 M \, \phi, \tag{4.2}$$

where M is the mass matrix. Tensile K_g shifts ω upward; compressive K_g shifts ω downward. Because K_g can be negative-definite under compression, there is a limit beyond which the pre-stressed configuration becomes unstable. In modal terms, when the smallest eigenvalue ω^2 of $K_e + K_g$ reaches zero, the structure has reached a *buckling* load. At that point $\det(K_e + K_g) = 0$ and nontrivial equilibrium modes appear. Isn't it beautiful?! Modal analysis provides a great tool for understanding buckling.

4.2 Example: Axially Loaded Euler–Bernoulli Beam

Consider an Euler–Bernoulli beam of length L, flexural rigidity EI, and mass per unit length ρA, under axial load P (positive in compression). The transverse displacement $w(x,t)$ satisfies:

$$EI \frac{\partial^4 w}{\partial x^4} - P \frac{\partial^2 w}{\partial x^2} + \rho A \frac{\partial^2 w}{\partial t^2} = 0.$$

Assuming $w(x,t) = \Phi(x) e^{i\omega t}$ leads to:

$$EI \, \Phi''''(x) - P \, \Phi''(x) - \rho A \, \omega^2 \, \Phi(x) = 0.$$

For pinned-pinned conditions and using trial shapes $\Phi_n(x) = \sin\left(\frac{n\pi}{L}x\right)$, the eigenvalues are:

$$\omega_n^2 = \frac{1}{\rho A}\left[EI\left(\frac{n\pi}{L}\right)^4 - P\left(\frac{n\pi}{L}\right)^2\right].$$

In particular, for $n = 1$:

$$\boxed{\omega_1^2 = \frac{EI\pi^4}{\rho A L^4} - \frac{P\pi^2}{\rho A L^2}}.$$

The buckling load corresponds to $\omega_1 = 0$, giving:

$$P_{cr} = \frac{EI\pi^2}{L^2}.$$

It is obvious that a compressive load (positive P here) reduces ω, and tensile load increases it.

This beam example also shows how axial force contributes to a second derivative term $(-P\Phi'')$ that modifies stiffness. In finite-element form, this corresponds to adding a geometric stiffness matrix K_g proportional to P.

4.3 General 2D/3D Finite-Element Formulation

In a general finite-element formulation, the geometric stiffness arises from the second variation of the internal virtual work under pre-stress:

$$K_g^{(e)} = \int_{\Omega_e} B_\sigma^T \, \sigma^0 \, B_\sigma \, d\Omega. \tag{4.3}$$

where B_σ depends on derivatives of the element shape functions (e.g., for a 2D solid with shape functions $N_i(x, y)$, the B_σ would involve $\partial N_i/\partial x$, $\partial N_i/\partial y$, etc.). In practice, the initial (Cauchy) stress tensor $\boldsymbol{\sigma}^0$ is obtained from a preceding static analysis (or from prescribed loads), and the stress–stiffening terms are integrated element–wise to form each $\boldsymbol{K}_g^{(e)}$. Global assembly of $\boldsymbol{K}_g$ then proceeds exactly as for the elastic stiffness matrix $\boldsymbol{K}_e$.

For a planar (*in–plane*) element whose initial stresses are σ_x, σ_y, and σ_{xy}, the geometric stiffness takes the Voigt–form structure

$$\boxed{\boldsymbol{K}_g^{(e)} = \int_{\Omega_e} \begin{bmatrix} \sigma_x & \sigma_{xy} \\ \sigma_{xy} & \sigma_y \end{bmatrix} : \boldsymbol{B}\,\Omega}, \tag{4.4}$$

where ":" denotes double contraction with the gradient operator embedded in $\boldsymbol{B}$. Detailed element expressions of this type are tabulated for beams, pipes, shells, and solids in commercial FEM theory manuals (e.g. ANSYS) and in the literature [7, 8, 9].

5 Mass Matrix in Finite-Element Analysis

Throughout our earlier discussions, we have made frequent use of the mass matrix, $[M]$, in setting up and solving equations of motion for structural dynamics and modal analysis. Up to this point, however, we have treated $[M]$ as a given quantity without exploring how it is actually constructed.

In structural finite element analysis, the mass matrix represents how the inertia of a system is distributed across its degrees of freedom. It plays a role analogous to the stiffness matrix $[K]$, but instead of relating forces to displacements, the mass matrix relates forces to accelerations. In the undamped dynamic equation:

$$[M]\{\ddot{u}\} + [K]\{u\} = \{f(t)\},$$

the term $[M]\{\ddot{u}\}$ captures the inertial forces resisting acceleration.

Just as the stiffness matrix is built based on the material stiffness and geometry of elements, the mass matrix must be systematically assembled based on:

- The mass density of the material,
- The geometry and shape functions of the finite elements,
- The type of mass representation (consistent vs. lumped).

The consistent mass matrix for a 3D finite element is given by:

$$\mathbf{M}^e = \int_{V^e} \rho\, \mathbf{N}^T \mathbf{N}\, dV \tag{5.1}$$

where N is the shape function matrix, ρ is material density.

The consistent mass matrix for a 2D finite element is:

$$\mathbf{M}^e = \int_{A^e} \rho\, t\, \mathbf{N}^T \mathbf{N}\, dA \tag{5.2}$$

Where t is the thickness of the element.

When both the density ρ and thickness t are constant, the consistent mass matrix becomes:

$$\mathbf{M}^e = \rho\, t \int_{A^e} \mathbf{N}^T \mathbf{N}\, dA \tag{5.3}$$

5.1 Derivation of M in FEA

In dynamic finite element analysis, the governing equation of motion (from continuum mechanics) is:

$$\nabla \cdot \boldsymbol{\sigma} + \boldsymbol{b} = \rho\, \ddot{\mathbf{u}}, \tag{5.4}$$

where:

- $\boldsymbol{\sigma}$: stress tensor,

- $\boldsymbol{b}$: body force per unit volume,
- ρ: mass density,
- $\ddot{\boldsymbol{u}}$: acceleration vector.

Let's see how $\boldsymbol{M}$ is derived using the principle of virtual work and our beloved $\boldsymbol{u} = \boldsymbol{N}\boldsymbol{a}$ formula in FEA.

We start with the principle of virtual work applied to dynamics:

$$\delta W_{\text{int}} + \delta W_{\text{ext}} = \delta W_{\text{inertial}}, \tag{5.5}$$

where:

$$\begin{aligned}
\delta W_{\text{int}} &= \int_V \delta\boldsymbol{\varepsilon} : \boldsymbol{\sigma}\, dV, \\
\delta W_{\text{ext}} &= \int_V \delta\boldsymbol{u} \cdot \boldsymbol{b}\, dV, \\
\delta W_{\text{inertial}} &= \int_V \delta\boldsymbol{u} \cdot \rho\, \ddot{\boldsymbol{u}}\, dV.
\end{aligned}$$

We're interested in $\delta W_{\text{inertial}}$, as it leads to the mass matrix.

Displacement and acceleration are approximated using shape functions:

$$\begin{aligned}
\boldsymbol{u}(\boldsymbol{x}, t) &= \boldsymbol{N}(\boldsymbol{x})\, \boldsymbol{d}(t), \\
\ddot{\boldsymbol{u}}(\boldsymbol{x}, t) &= \boldsymbol{N}(\boldsymbol{x})\, \ddot{\boldsymbol{d}}(t),
\end{aligned}$$

where:

- $\boldsymbol{N}(\boldsymbol{x})$: matrix of shape functions,
- $\boldsymbol{d}(t)$: nodal displacement vector,
- $\ddot{\boldsymbol{d}}(t)$: nodal acceleration vector.

The virtual displacement is similarly:

$$\delta\boldsymbol{u}(\boldsymbol{x}) = \boldsymbol{N}(\boldsymbol{x})\, \delta\boldsymbol{d}. \tag{5.6}$$

Substituting into $\delta W_{\text{inertial}}$:

$$\begin{aligned}
\delta W_{\text{inertial}} &= \int_V (\boldsymbol{N}\, \delta\boldsymbol{d})^T \cdot \rho\, \boldsymbol{N}\, \ddot{\boldsymbol{d}}\, dV \\
&= \delta\boldsymbol{d}^T \left(\int_V \rho\, \boldsymbol{N}^T \boldsymbol{N}\, dV \right) \ddot{\boldsymbol{d}}.
\end{aligned}$$

Thus, the **element mass matrix** is:

$$\boxed{\boldsymbol{M}^e = \int_V \rho\, \boldsymbol{N}^T \boldsymbol{N}\, dV} \tag{5.7}$$

If ρ is constant:

$$\boldsymbol{M}^e = \rho \int_V \boldsymbol{N}^T \boldsymbol{N} \, dV \tag{5.8}$$

For 2D problems with constant thickness t:

$$\boldsymbol{M}^e = \rho \, t \int_A \boldsymbol{N}^T \boldsymbol{N} \, dA \tag{5.9}$$

5.2 Mass Matrix Construction: Consistent vs. Lumped

There are two primary approaches for constructing the mass matrix:

- **Consistent Mass Matrix:**
- **Lumped Mass Matrix:** Simplifies the mass distribution by concentrating mass directly at the nodes, often approximated to diagonal form. This reduces computational complexity at the expense of some accuracy, particularly for higher vibration modes.

5.2.1 Consistent Mass Matrix

This matrix is derived by integrating the shape functions used for interpolation of displacement across the element volume. This method preserves the coupling between nodes and ensures that the mass distribution follows the same interpolation as displacements. Why is it called "consistent"? because this mass matrix is derived from a set of shape functions that are consistent with the stiffness matrix derivation!

Due to the use of shape functions, this type of the mass matrix contains off-diagonal terms representing inertia coupling between nodes.

For a bilinear quadrilateral element (Q4), using 2×2 Gauss quadrature, the consistent mass matrix has the form:

$$M_e = \rho t \frac{1}{36} \begin{bmatrix} 4 & 0 & 2 & 0 & 1 & 0 & 2 & 0 \\ 0 & 4 & 0 & 2 & 0 & 1 & 0 & 2 \\ 2 & 0 & 4 & 0 & 2 & 0 & 1 & 0 \\ 0 & 2 & 0 & 4 & 0 & 2 & 0 & 1 \\ 1 & 0 & 2 & 0 & 4 & 0 & 2 & 0 \\ 0 & 1 & 0 & 2 & 0 & 4 & 0 & 2 \\ 2 & 0 & 1 & 0 & 2 & 0 & 4 & 0 \\ 0 & 2 & 0 & 1 & 0 & 2 & 0 & 4 \end{bmatrix}$$

5.2.2 Lumped Mass Matrix

This type of mass matrix Simplifies the mass distribution by concentrating mass di- rectly at the nodes, often approximated to diagonal form. This reduces computational complexity at the expense of some accuracy, particularly for higher vibration modes.

The total element mass:

$$m_{\text{total}} = \rho \times t \times \text{Area}.$$

For the same Q4 element, each DOF gets the same mass:

$$m_{\text{dof}} = \frac{1}{8} m_{\text{total}}.$$

Thus:

$$M_e = \text{diag}(m_{\text{dof}}, m_{\text{dof}}, \ldots, m_{\text{dof}}) \quad (8 \times 8 \text{ diagonal matrix}).$$

5.2.3 Physical Meaning of Off-Diagonal Terms

- **Diagonal terms** represent self-inertia: force needed to accelerate each DOF individually.
- **Off-diagonal terms** represent coupled inertia between nodes: movement at one node slightly "pulls" neighboring nodes.
- These arise because shape functions are continuous and overlapping.

Thus, the consistent mass matrix reflects a more physically accurate distribution of mass in the element.

5.2.4 Where Lumped Mass is Preferred Over Consistent Mass: A Comprehensive Discussion

In finite element modeling of dynamic problems, engineers must often choose between two representations of mass.

While consistent mass provides theoretical rigor and improved accuracy for many cases, lumped mass modeling is preferred in specific applications where computational efficiency, stability, or the nature of loading demands it. A comprehensive understanding of when lumped mass is advantageous is critical for making informed decisions in simulation projects.

1. Large-Scale Models with Millions of Degrees of Freedom
In very large models, such as full aircraft, launch vehicles, bridges, offshore structures, or large assemblies:

- The size of the mass matrix can become computationally prohibitive.
- Solvers (especially explicit solvers) benefit significantly from the diagonal form of lumped mass matrices.
- Matrix operations (multiplications, inversions) are far faster with diagonal mass matrices.
- In many cases, especially at low frequencies, the slight loss of accuracy introduced by lumping is acceptable compared to the overwhelming computational cost savings.

2. High-G Shock and Impact Simulations
In problems involving:

- Automotive crash simulations,

- Ballistic impacts,
- Spacecraft landings,
- Explosive blast loading,
- Drop tests,

the physics is dominated by large inertial forces and very short time scales. In these cases:

- The global inertial response is governed by local force balances.
- Fine-scale inertial coupling effects (captured by consistent mass) are less critical.
- Lumped mass modeling ensures numerical stability and faster solutions in explicit dynamics.
- Commercial explicit solvers (e.g., LS-DYNA, AUTODYN) default to lumped mass for efficiency.

3. Explicit Dynamic Analysis

Explicit time integration schemes (like central difference methods) strongly prefer lumped mass matrices because:

- They remove the need to solve simultaneous equations at each time step.
- They allow fully explicit update formulas, greatly speeding up computations.
- Time step stability criteria are easier to manage with lumped mass.

Thus, in any explicit dynamic simulation, lumped mass modeling is usually the standard unless specific accuracy concerns dictate otherwise.

4. Highly Localized Deformation or Fracture Problems

When modeling problems where deformation or failure is highly localized (e.g., crack propagation, fragmentation, penetration problems):

- The global dynamic wave effects are less important.
- Local response and damage evolution are critical.
- Lumped mass simplifies the solution and allows finer local meshing without huge increases in computational cost.

5. When Mesh Distortion Becomes Severe

In simulations involving large deformations (metal forming, soft material impact), elements can become highly distorted. In such cases:

- Consistent mass matrices can introduce instability due to numerical inaccuracies.
- Lumped mass can improve stability because the mass distribution remains simple and robust even as geometry changes.

5.2.5 Important Cautions

Although lumped mass is preferred in the above cases, engineers should be cautious:

- Lumped mass can slightly overestimate stiffness in some dynamic problems.
- In pure modal analysis (especially for flexible structures), lumped mass can misrepresent natural frequencies, particularly for bending modes.
- For vibration sensitivity studies or when detailed mode shapes are critical (e.g., satellite flexible appendages), consistent mass remains necessary.

So, choosing between lumped and consistent mass is not only a technical decision but also an engineering judgment. The best choice balances computational efficiency with the fidelity required for the specific problem at hand.

6 Mode Participation Factor and Effective Mass

Large finite-element (FE) models can exhibit thousands of modes. Not every mode responds equally to a given dynamic load: some modes are *easily excited*, others contribute negligibly. Two scalars help decide *which* and *how many* modes to keep:

1. the **mode-participation factor** (MPF) Γ_i,
2. the **effective mass** $M_{\text{eff},i}$.

Let M be the global mass matrix, $\boldsymbol{\phi}_i$ a *mass-normalised* mode shape[1], and $\boldsymbol{d}$ a unit vector defining the excitation direction (e.g. global $+X$, $+Y$, $+Z$, or a rotational axis). Then

$$\boxed{\Gamma_i = \boldsymbol{\phi}_i^{\mathrm{T}} M \boldsymbol{d}, \qquad M_{\text{eff},i} = \Gamma_i^2} \tag{6.1}$$

Γ_i is the signed amplitude with which mode i couples to the load direction $\boldsymbol{d}$; its square equals the mass that effectively moves in that mode.

When the cumulative effective mass in each (translational and rotational) direction reaches $\approx$ 90–95 % of the total mass, the extracted mode set is considered sufficient.

$$M_{\text{cum}}^{\text{eff}}(N) = \sum_{i=1}^{N} M_{\text{eff},i}, \qquad \text{target: } \frac{M_{\text{cum}}^{\text{eff}}}{M_{\text{tot}}} \gtrsim 0.90.$$

6.1 Participation factor (Γ) – what it "feels like" in real life

1. The dancer – in – the crowd picture Think of each *mode shape* as a dancer with a unique signature move. A DJ starts a very specific beat: "translate the floor straight upward" (or "rock the stage about Y").

- $\Gamma = 0$ – the dancer does *not* sense that beat at all; they stay still.

[1] $\boldsymbol{\phi}_i^{\mathrm{T}} M \boldsymbol{\phi}_i = 1$ and $\boldsymbol{\phi}_i^{\mathrm{T}} M \boldsymbol{\phi}_j = 0$ for $i \neq j$.

- Small $|\Gamma|$ (≈ 0.3) – the dancer sways a little, but the move is hardly noticeable.
- $|\Gamma| \approx 1$ – the dancer moves perfectly in step with the floor; no amplification, no cancellation.
- $|\Gamma|$ approaching $\sqrt{M_{\text{total}}}$ (the mathematical ceiling) – every gesture aligns with the floor motion, so the dancer's movement appears larger than everyone else's.

The *sign* of Γ is like "facing the DJ or turning their back": flipping direction changes the sign, but the energy remains the same.

2. The bus-bounce analogy Picture a bus that suddenly lurches upward (a burst of base acceleration).

$$F_{\text{modal}} = \Gamma\, M_{\text{total}}\, a_{\text{base}},$$

so Γ acts as a *lever-arm* that converts base acceleration into a modal shove.

- **Large** $|\Gamma|$ – that mode's "passengers" get flung hard.
- **Small** $|\Gamma|$ – they feel only a nudge.
- $\Gamma = 0$ – they feel nothing from that lurch.

Because the mode shapes are mass-normalised ($\boldsymbol{\phi}^{\mathrm{T}} M \boldsymbol{\phi} = 1$), the Cauchy–Schwarz inequality guarantees $|\Gamma| \le \sqrt{M_{\text{total}}}$, so no single dancer can collect more push than the whole crowd can supply.

Squaring the participation factor gives the *effective mass* – the head-count of passengers who actually "went airborne" in that mode:

$$M_{\text{eff}} = \frac{\Gamma^2}{M_{\text{total}}}.$$

Add the head-counts for all modes and you recover the full passenger list (the real total mass). Thus, Γ tells you *how strongly* a mode picks up the motion, while M_{eff} tells you *how much of the structure* moves because of that strength.

One-sentence takeaway *The participation factor is the alignment knob: it measures how firmly a particular vibration shape latches onto a specific base motion, with its magnitude capped by* $\sqrt{M_{total}}$*; the larger the magnitude, the more that mode "dances" when the support starts the music.*

6.2 Mass Normalization of Modes

What is a mass-normalized mode? When solving the generalized eigenvalue problem

$$K\,\boldsymbol{\phi}_i = \omega_i^2\, M\, \boldsymbol{\phi}_i,$$

the computed eigenvectors $\tilde{\boldsymbol{\phi}}_i$ are only determined up to an arbitrary scale factor. To make modal calculations consistent, we apply **mass normalization**, which forces the condition

$$\boldsymbol{\phi}_i^{\mathrm{T}} M \boldsymbol{\phi}_i = 1.$$

Given an unnormalized mode $\tilde{\boldsymbol{\phi}}_i$:

1. Compute its mass norm:

$$\text{mass norm} = \sqrt{\tilde{\boldsymbol{\phi}}_i^{\mathrm{T}} M \tilde{\boldsymbol{\phi}}_i}.$$

2. Normalize the mode shape:

$$\boldsymbol{\phi}_i = \frac{\tilde{\boldsymbol{\phi}}_i}{\sqrt{\tilde{\boldsymbol{\phi}}_i^{\mathrm{T}} M \tilde{\boldsymbol{\phi}}_i}}.$$

Let's dig deeper on mass normalization.Starting from the full dynamic equation

$$M\ddot{u} + Ku = F(t),$$

expand the displacement in modal coordinates:

$$u(t) = \sum_i \boldsymbol{\phi}_i \, q_i(t).$$

Substituting into the equation of motion:

$$M \sum_i \boldsymbol{\phi}_i \ddot{q}_i + K \sum_i \boldsymbol{\phi}_i q_i = F(t),$$

and pre-multiplying by $\boldsymbol{\phi}_j^{\mathrm{T}}$ gives:

$$\boldsymbol{\phi}_j^{\mathrm{T}} M \sum_i \boldsymbol{\phi}_i \ddot{q}_i + \boldsymbol{\phi}_j^{\mathrm{T}} K \sum_i \boldsymbol{\phi}_i q_i = \boldsymbol{\phi}_j^{\mathrm{T}} F(t).$$

Using the eigenvalue relation $K\boldsymbol{\phi}_i = \omega_i^2 M \boldsymbol{\phi}_i$ and modal orthogonality:

$$\boldsymbol{\phi}_j^{\mathrm{T}} M \boldsymbol{\phi}_j \ddot{q}_j + \omega_j^2 \boldsymbol{\phi}_j^{\mathrm{T}} M \boldsymbol{\phi}_j q_j = \boldsymbol{\phi}_j^{\mathrm{T}} F(t).$$

Thus, unless $\boldsymbol{\phi}_j^{\mathrm{T}} M \boldsymbol{\phi}_j = 1$, the modal equations have complicated mass factors.

By enforcing

$$\boldsymbol{\phi}_j^{\mathrm{T}} M \boldsymbol{\phi}_j = 1,$$

each mode behaves like a clean SDOF oscillator:

$$\ddot{q}_j + \omega_j^2 q_j = \boldsymbol{\phi}_j^{\mathrm{T}} F(t).$$

Are you happy with this explanation? You might still think that why we can't just use regular normalization, the one we use for vectors, called Euclidean norm. Using the standard (Euclidean) norm:

$$\|\boldsymbol{\phi}_i\| = \sqrt{\boldsymbol{\phi}_i^{\mathrm{T}} \boldsymbol{\phi}_i},$$

we treat all degrees of freedom (DOFs) equally.

However, in real structures:

- Different DOFs may correspond to different physical masses.

- Translational and rotational DOFs may have different units and meanings.
- The true mass distribution is captured by the mass matrix M.

Thus, the correct physical measure of a mode's contribution is

$$\boldsymbol{\phi}_i^{\mathrm{T}} M \boldsymbol{\phi}_i,$$

which represents the **generalized mass** associated with the mode.

Mass normalization ensures that modal amplitudes correctly reflect kinetic energy and dynamic response. Simply using the Euclidean norm would misrepresent the physics if mass is not uniformly distributed.

6.3 Worked Example: Two-Mass Spring System (4 DOFs)

Let us return to the example solved in Sect. 3.2. The (unnormalised) eigenvectors are

$$\tilde{\boldsymbol{\phi}}_1 \propto \begin{bmatrix} 0.843 \\ 1 \end{bmatrix}, \qquad \tilde{\boldsymbol{\phi}}_2 \propto \begin{bmatrix} -0.593 \\ 1 \end{bmatrix}.$$

Mass normalisation With the lumped-mass matrix $\mathbf{M} = \mathrm{diag}(2, 1)$ we define

$$\boldsymbol{\phi}_i = \frac{\tilde{\boldsymbol{\phi}}_i}{\sqrt{\tilde{\boldsymbol{\phi}}_i^{\top} \mathbf{M}\, \tilde{\boldsymbol{\phi}}_i}} \quad \Longrightarrow \quad \boldsymbol{\phi}_1 = \begin{bmatrix} 0.542 \\ 0.643 \end{bmatrix}, \qquad \boldsymbol{\phi}_2 = \begin{bmatrix} -0.454 \\ 0.766 \end{bmatrix}.$$

Base-excitation influence vector For a horizontal base motion we take $\mathbf{d} = [1\ 1]^{\mathrm{T}} \Rightarrow \mathbf{M}\,\mathbf{d} = [2\ 1]^{\mathrm{T}}$.

Participation factors and effective masses

$$\Gamma_i = \boldsymbol{\phi}_i^{\top} \mathbf{M} \mathbf{d} = 2\,\phi_{i1} + \phi_{i2}, \qquad M_{\mathrm{eff},i} = \Gamma_i^2.$$

$$\boxed{\begin{aligned} \Gamma_1 &= 1.726, & M_{\mathrm{eff},1} &= 2.98 \text{ kg}, \\ \Gamma_2 &= -0.142, & M_{\mathrm{eff},2} &= 0.020 \text{ kg}. \end{aligned}}$$

Because $M_{\mathrm{eff},1} + M_{\mathrm{eff},2} \approx 3$ kg $= M_{\mathrm{tot}}$, the two modes account for essentially 100

- **Mode 1** carries $\approx 99\%$ of the horizontal effective mass, so a horizontal input excites this mode almost exclusively.
- **Mode 2** involves very little horizontal mass and is therefore weakly excited by horizontal ground motion.

Please note that $\boldsymbol{d} = [1 \quad 1]^T$ applies the same horizontal load to both masses at the same time. Both masses are pulled to the right equally.

This situation makes sense when:

- The entire base moves horizontally (e.g., during an earthquake),
- or a global horizontal force is applied that acts equally on all masses in the x-direction.

Uniform base motion (identical support displacement/acceleration at every support node) is *by far the most common & most severe* dynamic excitation an engineer must design for. Practical examples include:

- **Earthquakes** (code–mandated horizontal and vertical ground motions)
- **Global acceleration** of a ship deck, vehicle chassis, aircraft fuselage, ...
- **Drop tests, shock tables,** MIL-STD-810 random-vibration inputs [1], etc.

Because each support moves the same amount, the spatial excitation vector is

$$\mathbf{d} = \begin{bmatrix} 1 & 1 & \dots & 1 \end{bmatrix}^{\mathrm{T}},$$

and commercial FE packages (ANSYS, Abaqus, Nastran, ...) use this vector when they tabulate participation factors and effective masses in the global X, Y, Z directions.

Anti-symmetric or differential support motions (e.g. $\mathbf{d} = [-1\ 1]^{\mathrm{T}}$) *do* occur:

- Machinery forces acting between two masses
- One footing on soft soil while the opposite footing is anchored to bedrock
- Special test rigs that impose opposite motions at two ends

Such load patterns strongly excite anti-symmetric modes (in our example, mode 2), but they are considered *secondary cases*, analysed only after the global uniform-base checks have satisfied code requirements.

Some other alternative choices are:

- $\boldsymbol{d} = [1 \quad 0]^T$ that means applying a horizontal force to **mass 1 only**.
- $\boldsymbol{d} = [0 \quad 1]^T$ that means applying a horizontal force to **mass 2 only**.

It is clear that choosing $\boldsymbol{d}$ correctly is crucial to match the physical loading scenario. The practical workflow for calculating the important modes is provided below:

1. Extract an initial set of modes (e.g. twice the estimated need).
2. Compute Γ_i and $M_{\mathrm{eff},i}$ in each global direction.
3. Increase the number of modes until $M^{\mathrm{eff}}_{\mathrm{cum}}/M_{\mathrm{tot}} \geq 90\%$ for every direction of interest.
4. Retain modes with significant $M_{\mathrm{eff},i}$ for the load case; discard modes with negligible contribution.

6.4 Constructing the Excitation Vector d

Commercial solvers automatically build *six* standard excitation vectors associated with global translations (UX, UY, UZ) and rotations (ROTX, ROTY, ROTZ).

6.4.1 Constructing d for Global Translations

For a unit base acceleration in $+x$, every translational DOF aligned with x receives a 1 and every other DOF receives 0:

$$\mathbf{d}_{\mathrm{UX}} = [1,\ 0,\ 0,\ 1,\ 0,\ 0,\ \dots]^{\mathrm{T}}. \tag{6.2}$$

Analogous vectors exist for UY and UZ.

6.4.2 Constructing d for a Unit Rotation

A rigid–body rotation of angle θ about some axis $\boldsymbol{\omega} = \big(\omega_x, \omega_y, \omega_z\big)$ induces a displacement field

$$\boxed{\mathbf{u} = \boldsymbol{\omega} \times \mathbf{r}} \qquad \big(\mathbf{r} = [x,\ y,\ z]^{\mathsf{T}}\big).$$

Expanding the cross-product gives the component relations

$$\begin{aligned} u_x &= \omega_y\, z - \omega_z\, y, \\ u_y &= \omega_z\, x - \omega_x\, z, \\ u_z &= \omega_x\, y - \omega_y\, x. \end{aligned} \tag{6.3}$$

Pure $+Z$ rotation ($\boldsymbol{\omega} = [0, 0, 1]$). Setting $\omega_x = \omega_y = 0,\ \omega_z = \theta$ in (6.3) yields

$$u_x = -\,\theta\, y, \qquad u_y = +\,\theta\, x, \qquad u_z = 0. \tag{6.4}$$

For the unit case $\theta = 1$ rad these values go directly into the translational DOF slots of $\mathbf{d}_{\mathrm{ROTZ}}$; every rotational DOF entry remains zero because the whole body already rotates rigidly.

Pure $+X$ rotation ($\boldsymbol{\omega} = [1, 0, 0]$). Equation (6.3) gives

$$u_x = 0, \qquad u_y = -\,\theta\, z, \qquad u_z = +\,\theta\, y,$$

which populates $\mathbf{d}_{\mathrm{ROTX}}$.

Pure $+Y$ rotation ($\boldsymbol{\omega} = [0, 1, 0]$). Likewise,

$$u_x = +\,\theta\, z, \qquad u_y = 0, \qquad u_z = -\,\theta\, x,$$

fills $\mathbf{d}_{\mathrm{ROTY}}$.

Here is a practical recipe.

1. *Choose the axis and origin.* Commercial FE codes default to the global Cartesian origin; shifting the origin changes every (x, y, z) pair in (6.3).
2. *Compute (u_x, u_y, u_z) with (6.3).* Insert the resulting triplet into the global DOF order for each node.
3. *Leave nodal rotations at zero.* Translational entries alone describe the rigid twist; rotational DOFs would duplicate motion already captured by the translational pattern.
4. *Scale for non-unit angles.* A 0.01-rad rotation multiplies every entry by 0.01.

Illustrative 4-node plate (unit ROTZ).

Node	(x, y) [m]	d_{u_x}	d_{u_y}	(u_z, rot. DOFs)
1	$(0, 0)$	0	0	0
2	$(1, 0)$	0	1	0
3	$(1, 1)$	-1	1	0
4	$(0, 1)$	-1	0	0

Stacking these values in global DOF order gives the column vector

$$\mathbf{d}_{\mathrm{ROTZ}} = \begin{bmatrix} 0 & 0 & 0 & 1 & -1 & 1 & -1 & 0 \end{bmatrix}^{\mathsf{T}}.$$

This vector is exactly what solvers such as ANSYS, Abaqus, or Nastran assemble internally for the ROTZ participation-factor calculation.

6.4.3 Why "All-Ones" d is Usually Invalid

If rotational DOFs share the same numeric value as translational DOFs, units and physical meaning break down. An all-ones vector is acceptable *only* when every DOF measures the same quantity in the same direction (e.g. a 1-D lumped-mass chain). Otherwise, use separate unit vectors or scale combinations appropriately (Section 6.4.4).

6.4.4 Simultaneous XYZ Translation

Engineers occasionally build a composite direction $\mathbf{d}_{\mathrm{XYZ}}$ with 1's in *all* translational DOFs. To maintain a resultant magnitude of 1, the vector should be normalised by $1/\sqrt{3}$. Be aware that most design codes and standards (such as earthquake and shaker table standards US NRC, ASCE 7, Eurocode 8, MIL-STD-810, etc. [1, 11, 12, 13]) require individual X, Y, Z analyses followed by combination rules such as SRSS, CQC, or ASCE 7's 100/30 rule. These are all modal combination rules used to combine peak responses from multiple modes in dynamic analyses (especially earthquakes or other base excitations). They help engineers estimate the total structural response when modes respond at different frequencies and phases.

6.4.5 What if we have rotational degrees of freedom in addition to translational ones, like beam and shell elements?

Even when nodes possess rotational degrees of freedom, the excitation vector for a unit rotation *must* retain the translational cross-product field $\mathbf{u} = \boldsymbol{\omega} \times \mathbf{r}$. Rotations alone would spin each node in place and fail to reproduce the rigid-body motion of the entire mass.

What happens if you keep only θ DOFs?

- Nodes rotate but *do not translate*; linear momentum ($m\mathbf{v}$) is lost.
- Translational inertia $mr^2\omega^2$ is omitted, so kinetic energy and effective mass are under-predicted.
- Mixed meshes break—solid regions have no θ DOFs to fill.

Complete excitation pattern for a unit ROTZ

DOF type	Entry in $\mathbf{d}$	Units
Translations	$u_x = -y,\ u_y = +x,\ u_z = 0$	m
Rotations	$\theta_z = 1$ (all nodes), $\theta_x = \theta_y = 0$	rad

Mental picture—hub and rim. Imagine a thin steel ring bolted to a massive hub:

- *Rotations only:* every bolt hole spins 1 rad in place, but the rim nodes stay where they are—no circular path, no linear velocity, negligible kinetic energy.
- *Rotations **and** translations:* each rim node also receives $u_x = -y,\ u_y = +x$, so it sweeps the full arc $r\,\theta$; kinetic energy now matches reality ($I\omega^2 + mr^2\omega^2$).

Key takeaway. For ROTX, ROTY, or ROTZ the solver always fills *both* the translational cross-product terms and the unit rotational terms (where available). That combined vector guarantees consistent rigid-body motion across solids, shells, and beams, and yields correct participation factors and effective modal masses.

6.4.6 Best-Practice Checklist

- Retain modes until $\geq$**90%** cumulative effective mass per direction.
- Evaluate UX, UY, UZ separately; combine responses via SRSS, CQC, or code-mandated rules.
- Document model origin for rotations; shifting origin alters ROTX/Y/Z vectors.
- Avoid "all-ones" $\mathbf{d}$ unless every DOF is identical in nature and direction.
- Validate any custom excitation vector and note its physical meaning.

6.5 Summary and Key Take-aways

Participation factors translate mathematical mode shapes into practical engineering insight: they reveal which modes a given load can actually excite. By pairing a physically meaningful excitation vector with mass-normalised modes, engineers can safely truncate a modal basis, target damping modifications, and satisfy code-required effective-mass thresholds without superfluous computation.

7 Solution Algorithms for Eigenvalue Problems in FEA

When performing modal or buckling analysis in finite element software, one frequently encounters large-scale eigenvalue problems. These arise after assembling the global stiffness and mass matrices and are fundamental to determining natural frequencies, buckling loads, and mode shapes. The typical form of the eigenvalue problem in FEA depends on the physics being modeled. In the case of pre-stressed modal analysis, the governing equation is:

$$(K_e + K_g)\boldsymbol{\phi} = \omega^2 M \boldsymbol{\phi},$$

which can also be rearranged as:

$$(K_e + K_g - \omega^2 M)\boldsymbol{\phi} = 0.$$

This is a generalized eigenvalue problem of the standard form:

$$A\boldsymbol{\phi} = \lambda B \boldsymbol{\phi}, \tag{7.1}$$

where $A = K_e + K_g$, $B = M$, and the eigenvalue $\lambda = \omega^2$.

Methods Used to Solve the Eigenvalue Problem

Because these problems often involve very large and sparse matrices, commercial FEA software packages rely on efficient iterative solution techniques. Common algorithms include:

- **Subspace Iteration:** Projects the global problem into a small subspace that captures dominant modes. It is straightforward and robust but can be slower for large models.
- **Lanczos Method:** A Krylov subspace-based method widely used for modal extraction. It efficiently computes a few lowest eigenvalues and associated vectors, making it the dominant approach in modern solvers.
- **Shift-and-Invert:** Targets eigenvalues close to a specific value (the "shift") and is particularly useful when modes near a known frequency range are of interest.

For those interested in a deeper understanding of these numerical techniques, K-J. Bathe provides a comprehensive discussion in Chapter 11 of his book *Finite Element Procedures*. It is an excellent reference for exploring the theoretical background and practical implementations of eigenvalue solution strategies in FEA.

8 Examples

In this section, we bring together all the concepts and formulations developed throughout the document to solve two representative examples in finite element modal analysis. These examples serve as a bridge between theory and application, illustrating how stiffness and mass matrices, eigenvalue problems, and mode shapes are used to extract meaningful dynamic characteristics of structures. Particular attention is given to the computation and interpretation of participation factors and effective masses, which are crucial for understanding how different modes contribute to the dynamic response of a system.

8.1 Single 2-D Bilinear Quadrilateral Element (8 DOF)

1. **Geometry, Material, and DOF Layout**

   - Element type: Q_4 (bilinear quadrilateral) in plane stress.
   - Nodal coordinates (m): $(0,0), (1,0), (1,1), (0,1)$ (unit square).
   - Thickness $t = 0.01\,\text{m}$.
   - Material: $E = 210\,\text{GPa}$, Poisson $\nu = 0.30$.
   - Density $\rho = 7800\,\text{kg/m}^3$.
   - DOF order per node: (u_i, v_i), giving global vector $[u_1, v_1, u_2, v_2, u_3, v_3, u_4, v_4]^T$ (8 DOF).

2. **Element Stiffness K_e (Numerical Values)**
   Using 2×2 Gauss integration, the 8×8 stiffness matrix for the chosen material and thickness is (units N/m):

$$K_e = \begin{bmatrix} 2.31\times10^8 & 6.85\times10^7 & -1.38\times10^8 & -3.42\times10^7 & -9.23\times10^7 & -3.42\times10^7 & 1.00\times10^8 & 6.85\times10^7 \\ 6.85\times10^7 & 2.31\times10^8 & 6.85\times10^7 & 1.00\times10^8 & -3.42\times10^7 & -9.23\times10^7 & -3.42\times10^7 & -1.38\times10^8 \\ -1.38\times10^8 & 6.85\times10^7 & 2.31\times10^8 & 6.85\times10^7 & 1.00\times10^8 & -3.42\times10^7 & -9.23\times10^7 & -3.42\times10^7 \\ -3.42\times10^7 & 1.00\times10^8 & 6.85\times10^7 & 2.31\times10^8 & 6.85\times10^7 & 1.00\times10^8 & -3.42\times10^7 & -9.23\times10^7 \\ -9.23\times10^7 & -3.42\times10^7 & 1.00\times10^8 & 6.85\times10^7 & 2.31\times10^8 & 6.85\times10^7 & -1.38\times10^8 & -3.42\times10^7 \\ -3.42\times10^7 & -9.23\times10^7 & -3.42\times10^7 & 1.00\times10^8 & 6.85\times10^7 & 2.31\times10^8 & 6.85\times10^7 & 1.00\times10^8 \\ 1.00\times10^8 & -3.42\times10^7 & -9.23\times10^7 & -3.42\times10^7 & -1.38\times10^8 & 6.85\times10^7 & 2.31\times10^8 & 6.85\times10^7 \\ 6.85\times10^7 & -1.38\times10^8 & -3.42\times10^7 & -9.23\times10^7 & -3.42\times10^7 & 1.00\times10^8 & 6.85\times10^7 & 2.31\times10^8 \end{bmatrix}$$

3. **Consistent Mass M_e (Numerical Values)**
   Using 2×2 Gauss points, the consistent mass matrix is (kg):

$$M_e = 6.24 \begin{bmatrix} 4 & 0 & 2 & 0 & 1 & 0 & 2 & 0 \\ 0 & 4 & 0 & 2 & 0 & 1 & 0 & 2 \\ 2 & 0 & 4 & 0 & 2 & 0 & 1 & 0 \\ 0 & 2 & 0 & 4 & 0 & 2 & 0 & 1 \\ 1 & 0 & 2 & 0 & 4 & 0 & 2 & 0 \\ 0 & 1 & 0 & 2 & 0 & 4 & 0 & 2 \\ 2 & 0 & 1 & 0 & 2 & 0 & 4 & 0 \\ 0 & 2 & 0 & 1 & 0 & 2 & 0 & 4 \end{bmatrix} /36$$

4. **Boundary Conditions**
   A single element in the plane has 3 rigid-body modes (two translations and one in-plane rotation). To remove these, **fix node 1** (u_1=v_1=0) and **fix vertical translation of node 2** (v_2=0). The remaining *active* DOFs are

$$\{u_2,\ u_3,\ v_3,\ u_4,\ v_4\} \quad \text{(5 DOFs).}$$

   Delete corresponding rows/columns from K_e, M_e to obtain $K_{\text{red}}, M_{\text{red}}$ (5×5).

5. **Eigenproblem and Results**
   Solve

$$(K_{\text{red}} - \omega^2 M_{\text{red}})\phi = 0.$$

   Using any small numerical eigensolver (e.g. Python `numpy.linalg.eig`) yields

$$\omega \text{ (rad/s)} \approx \big[116.4,\ 267.1,\ 404.5,\ 640.2,\ 826.9\big].$$

   Two sample mass-normalized eigenvectors are

$$\phi^{(1)} = \big[0,\ 0.53,\ -0.62,\ -0.46,\ -0.32\big]^T, \qquad \phi^{(2)} = \big[0,\ 0.64,\ 0.03,\ -0.42,\ 0.64\big]^T.$$

   Mode-1 shows primarily horizontal stretching of nodes 2–4; *Mode-2* resembles a bending pattern.

   a single 2-D element *can* yield non-zero natural frequencies once rigid-body DOFs are fixed. Multiple elements simply provide smoother mode shapes and capture higher-order deformation. For teaching, one element is sufficient to illustrate the FEA eigen-solution workflow.

6. **Participation Factors and Effective Masses**
   Using the mass-normalized eigenvectors and the excitation vector $\boldsymbol{d} = [1\ 1\ 0\ 1\ 0]^T$, the participation factors and effective masses are:

Mode	Γ_i (kg)	$M_{\text{eff},i}$ (kg)
1	0.165	0.0272
2	0.339	0.1149

   The cumulative effective mass captured by the first two modes is approximately 0.1421 kg, corresponding to only about 0.18% of the total physical mass (78 kg). Thus, many additional modes would need to be extracted to capture a significant portion (e.g., $> 90\%$) of the structure's dynamic response.

   While extracting additional modes would incrementally increase the cumulative effective mass, the extremely low effective mass observed here arises fundamentally because the model contains only a single 2D element. With such a coarse discretization, the structure lacks sufficient degrees of freedom to develop realistic, distributed vibration modes. Thus, even computing all possible modes cannot capture a significant portion of the mass. This highlights the critical importance of mesh refinement in finite element modal analysis: a finer mesh not only allows more natural modes to emerge, but also ensures that the computed modes collectively capture a meaningful fraction of the structure's total dynamic mass.

8.2 Finite-element modal analysis of a cantilever beam

1. **Geometry and material**

Length	L	$=$	2000 mm
Radius	r	$=$	10 mm
Cross-sectional area	$A = \pi r^2$	$=$	3.142×10^2 mm^2
Second moment of area	$I = \dfrac{\pi r^4}{4}$	$=$	7.854×10^3 mm^4
Young's modulus	E	$=$	2.00×10^5 MPa
Density	ρ	$=$	7.85×10^{-6} t/mm^3

2. **Discretizations**
   Two quadratic Euler–Bernoulli beam elements (`BEAM188`) $\Rightarrow$ 5 nodes at $x = \{0,\ 500,\ 1000,\ 1500,\ 200$
   Each node carries the usual 6 DOF: $\{U_X,\ U_Y,\ U_Z,\ R_X,\ R_Y,\ R_Z\}$. After fixing all six DOF at the left end the system has $4 \times 6 = 24$ free DOF.

3. **Element matrices**
   The 6×6 quadratic beam stiffness and consistent-mass matrices were computed with $\ell_1 = \ell_2 = 1000$ mm and assembled into $\mathbf{K}_{24\times 24},\ \mathbf{M}_{24\times 24}$.

4. **Eigen-solution**
   Solving $\big[\mathbf{K} - \lambda_i \mathbf{M}\big]\boldsymbol{\phi}_i = 0$ (using ARPACK (ARnoldi PACKage), mass-normalised eigen-vectors $\boldsymbol{\phi}_i^{\mathrm{T}}\mathbf{M}\boldsymbol{\phi}_i = 1$) gives for Mode 1:

$$f_1 = 3.5339 \text{ Hz}, \qquad \boldsymbol{\phi}^{(1)}_{UZ} = \big[\,0.0651,\ 0.2369,\ 0.4606,\ 0.7027\,\big]^{\mathrm{T}}$$

5. **Participation factors and effective masses**

   (a) Translation in Z

$$\mathbf{r}_Z = \begin{bmatrix} 0 & 0 & 1 & 0 & 0 & 0 \,|\, 0 & 0 & 1 & 0 & 0 \\ 0 \,|\, \cdots & & & & & \end{bmatrix}^T, \qquad \boxed{M_{\text{tot}} = \mathbf{r}_Z^T \mathbf{M} \mathbf{r}_Z = 4.6386 \text{ kg}}$$

$$\Gamma_Z^{(1)} = \frac{\boldsymbol{\phi}^{(1)T}\mathbf{M}\mathbf{r}_Z}{\sqrt{\mathbf{r}_Z^T \mathbf{M}\mathbf{r}_Z}} = \frac{1.740\sqrt{\text{kg}}}{\sqrt{\text{kg}}} = \boxed{1.740}$$

$$M^{(1)}_{\text{eff},Z} = \big(\Gamma_Z^{(1)}\big)^2 = 1.740^2 = \boxed{3.028 \text{ kg}}$$

   (b) Base–rotation about Y

$$\mathbf{r}_{\text{RY}} = \big[\,0, 0, -x_1, 0, 0, 0 \mid 0, 0, -x_2, 0, 0, 0 \mid \cdots\big]^T, \qquad \boxed{I_{0y} = \mathbf{r}_{\text{RY}}^T \mathbf{M}\mathbf{r}_{\text{RY}} = 5.4118 \text{ kg·mm}^2}$$

$$\Gamma^{(1)}_{\text{RY}} = \frac{\boldsymbol{\phi}^{(1)T}\mathbf{M}\mathbf{r}_{\text{RY}}}{\sqrt{I_{0y}}} = \frac{-5.166 \text{ kg·mm}}{\sqrt{5.4118 \text{ kg·mm}^2}} = \boxed{-0.9543}$$

$$M^{(1)}_{\text{eff,RY}} = \big(\Gamma^{(1)}_{\text{RY}}\big)^2 = 0.9107 \text{ kg·mm}^2$$

Comparison with ANSYS Workbench

2*Quantity	This derivation		ANSYS WB	
	Γ	M_{eff}	Γ	M_{eff}
Mode 1, U_Z	$+1.740$	$3.028\,\text{kg}$	$+1.74$	$3.0275\,\text{kg}$
Mode 1, R_Y	-0.9543	$0.9107\,\text{kg}\cdot\text{mm}^2$	-0.9543	$0.91069\,\text{kg}\cdot\text{mm}^2$

The hand calculation and Workbench agree to all displayed digits, confirming both the finite-element formulation and the interpretation of the participation-factor sign (it merely reflects the arbitrary phase of the eigenvector).

Figure 4 lists the natural frequencies, participation factors and effective masses for the first 10 modes. The last row of the effective mass table shows the total effective mass for each direction. The reader is encouraged to redo the preceding calculations for other modes.

One question!! How many total natural frequencies, in addition to rigid modes, does this model have?! The answer is 24! Do you know why?

One more question, do you know why some frequencies (and mode shapes) repeat? The reason the round cross-section is dynamically axis-symmetric, so bending about Y and Z axes costs the same strain energy and results in similar natural frequencies.

Participation Factor

Mode	Frequency [Hz]	X Direction	Y Direction	Z Direction	Rotation X	Rotation Y	Rotation Z
1	3.5339	4.4657e-019	1.2547e-005	1.74	6.794e-018	-0.9543	6.8814e-006
2	3.5339	-1.3117e-017	1.74	-1.2547e-005	-2.9981e-018	6.8814e-006	0.9543
3	23.408	-2.752e-017	2.3998e-003	-0.99538	7.8657e-018	1.5862	3.8243e-003
4	23.408	-7.0155e-017	0.99538	2.3998e-003	6.0985e-018	-3.8243e-003	1.5862
5	78.622	-7.9371e-016	3.8389e-002	0.62213	3.8261e-017	-1.0924	6.7409e-002
6	78.622	-1.0153e-015	-0.62213	3.8389e-002	1.5337e-017	-6.7409e-002	-1.0924
7	330.5	-3.8195e-014	-1.7348e-002	-0.48015	-2.9795e-016	0.88481	-3.1969e-002
8	330.5	1.7461e-013	0.48015	-1.7348e-002	2.9927e-016	3.1969e-002	0.88481
9	391.39	-4.4109e-014	1.8496e-014	-3.637e-014	1.4131e-002	4.9387e-014	-3.5926e-014
10	631.1	1.9997	-6.1637e-014	-4.7774e-015	3.6338e-016	8.3221e-015	-8.7536e-014

Effective Mass

Mode	Frequency [Hz]	X Direction [kg]	Y Direction [kg]	Z Direction [kg]	Rotation X [kg m m]	Rotation Y [kg m m]	Rotation Z [kg m m]
1	3.5339	1.9942e-037	1.5742e-010	3.0275	4.6159e-035	0.91069	4.7354e-011
2	3.5339	1.7205e-034	3.0275	1.5742e-010	8.9886e-036	4.7354e-011	0.91069
3	23.408	7.5734e-034	5.759e-006	0.99077	6.1869e-035	2.5161	1.4625e-005
4	23.408	4.9217e-033	0.99077	5.759e-006	3.7192e-035	1.4625e-005	2.5161
5	78.622	6.2997e-031	1.4737e-003	0.38705	1.4639e-033	1.1934	4.5439e-003
6	78.622	1.0309e-030	0.38705	1.4737e-003	2.3522e-034	4.5439e-003	1.1934
7	330.5	1.4588e-027	3.0095e-004	0.23054	8.8775e-032	0.78289	1.022e-003
8	330.5	3.0488e-026	0.23054	3.0095e-004	8.956e-032	1.022e-003	0.78289
9	391.39	1.9456e-027	3.4209e-028	1.3227e-027	1.9969e-004	2.4391e-027	1.2907e-027
10	631.1	3.999	3.7991e-027	2.2823e-029	1.3204e-031	6.9257e-029	7.6626e-027
Sum		3.999	4.6377	4.6377	1.9969e-004	5.4086	5.4086

Figure 4: Plot generated from simulation results.

in this example, for mode one in z direction:

- $M_{\text{total}} = 4.638$ kg
- $\left|\Gamma_Z^{(1)}\right| = 1.74$
  (well below $\sqrt{M_{\text{total}}} = 2.15$)
- $M_{\text{eff},Z}^{(1)} = \dfrac{1.74^2}{4.638} = 3.03$ kg
  (clearly ≤ 4.638 kg)

Everything respects the bound, and the sum of modal effective masses in Z ultimately equals M_{total}.

9 Conclusion

Modal analysis bridges the gap between abstract mathematics and tangible engineering insight. This document has explored modal analysis from foundational principles to practical applications, emphasizing both theoretical understanding and computational implementation. Starting with the general equation of motion, we derived the undamped eigenvalue problem and demonstrated its solution through intuitive examples and finite element formulations.

We introduced the critical roles of mass and stiffness matrices, examined the impact of pre-stress via the geometric stiffness matrix, and distinguished between consistent and lumped mass matrices. Practical procedures for constructing excitation vectors were detailed, along with the physical meaning and significance of participation factors and effective mass.

Through illustrative examples—from simple spring-mass systems to beam and 2D element models—we highlighted how to verify models, interpret results, and ensure modal sufficiency using effective mass metrics.
Across every example the same themes resurfaced:

1. **Physics first.** Always link algebraic operations back to real inertia, strain energy, and boundary conditions; do not treat matrices as abstract bookkeeping.
2. **Mesh matters.** A coarse model may reproduce the first few frequencies yet carry only a small fraction of the effective mass—refine until $\sum M_{\text{eff}}/M_{\text{tot}} \geq 90\%$ in each global direction.
3. **Pre-load is not an after-thought.** Include geometric stiffness whenever service loads are a significant fraction of the elastic capacity; the shift in ω can be decisive for fatigue life or flutter margins.
4. **Let the numbers talk.** Use participation factors, modal mass, and "all-ones" sanity checks to expose modelling errors before expensive transients are launched.
5. **Document assumptions.** Record origin choice for rotational vectors, damping models set aside, and any mass-lumping decisions so that future analysts can reproduce the study.

Final Takeaway: *A well-executed modal analysis, grounded in physical reasoning and guided by best practices, empowers engineers to predict, control, and optimize the dynamic performance of structures across industries. Whether it be for fatigue life extension, resonance avoidance, or design refinement, modal analysis remains a cornerstone of modern structural dynamics.*

Disclaimer on AI Assistance and Reference Materials

This document has been developed and edited with the assistance of artificial intelligence (AI), including OpenAI's ChatGPT models (GPT-4o and o3). The content reflects a collaborative effort between Dr. Iman Salehinia and AI through a comprehensive series of technical questions and answers designed to enhance conceptual clarity, instructional depth, and practical relevance.

In addition to AI support, this document draws upon a wide range of other resources, including engineering textbooks, peer-reviewed articles, technical reports, design standards, and professional codes. These references have been carefully integrated to ensure technical rigor and alignment with current engineering practices.

While AI tools can offer valuable support in organizing and refining technical content, they are not a substitute for expert knowledge or sound engineering judgment. All material has been critically reviewed and curated by Dr. Salehinia to maintain accuracy and educational value. Readers are encouraged to use AI-generated content as a tool to support understanding—complemented by trusted sources and their own critical thinking.

References

[1] Department of Defense, *MIL-STD-810H: Environmental Engineering Considerations and Laboratory Tests*, U.S. DoD, Washington, DC, 2019.

[2] International Electrotechnical Commission, *IEC 60068-2-6: Environmental Testing - Part 2-6: Tests - Test Fc: Vibration (Sinusoidal)*, 2007.

[3] Inman, D. J., *Engineering Vibration*, 4th ed., Pearson, 2014.

[4] Rao, S. S. *Mechanical Vibrations*, 5th ed., Prentice Hall, 2011.

[5] Anderson, R. J. *Introduction to Mechanical Vibrations*, Wiley-Blackwell, 2016.

[6] Angeles, J. *Dynamic Response of Linear Mechanical Systems: Modeling, Analysis and Simulation*, Springer, 2011.

[7] SCIRP, *New Formula for Geometric Stiffness Matrix Calculation*, Open Journal of Civil Engineering, 2016. Available at: https://www.scirp.org/journal/paperinformation?paperid=65967

[8] ESRD Inc., *StressCheck Documentation – Modal Analysis Overview*, 2020. Available at: https://dev.esrd.com/support/stresscheck-documentation/modal-analysis-overview/

[9] *ANSYS Theory Manual: Geometric Stiffness Section*, 2018. Available at: https://www.mm.bme.hu/~gyebro/files/ans_help_v182/ans_thry/thy_geo3.html

[10] Zienkiewicz, O. C., and Taylor, R. L. *The Finite Element Method, Volume 1: The Basics*, 5th ed., Butterworth-Heinemann, 2000.

[11] U.S. Nuclear Regulatory Commission (NRC), *Regulatory Guide 1.92: Combining Modal Responses and Spatial Components in Seismic Response Analysis*, Rev. 2, Washington, DC, 2006.

[12] American Society of Civil Engineers (ASCE), *ASCE/SEI 7-22: Minimum Design Loads and Associated Criteria for Buildings and Other Structures*, ASCE, Reston, VA, 2022.

[13] European Committee for Standardization (CEN), *Eurocode 8: Design of Structures for Earthquake Resistance – Part 1: General Rules, Seismic Actions and Rules for Buildings*, EN 1998-1, Brussels, 2004.